RM No. L8I30

NACA RM No. L8I30

NACA

RESEARCH MEMORANDUM

TRANSONIC-FLUTTER INVESTIGATION OF WINGS ATTACHED TO TWO LOW-ACCELERATION ROCKET-PROPELLED VEHICLES

By

Reginald R. Lundstrom, William T. Lauten, Jr., and Ellwyn E. Angle

Langley Aeronautical Laboratory
Langley Field, Va.

NATIONAL ADVISORY COMMITTEE FOR AERONAUTICS

WASHINGTON

November 23, 1948
Declassified December 14, 1953

NATIONAL ADVISORY COMMITTEE FOR AERONAUTICS

RESEARCH MEMORANDUM

TRANSONIC-FLUTTER INVESTIGATION OF WINGS ATTACHED TO TWO LOW-ACCELERATION ROCKET-PROPELLED VEHICLES

By Reginald R. Lundstrom, William T. Lauten, Jr., and Ellwyn E. Angle

SUMMARY

Two low-acceleration transonic-flutter test vehicles were launched and flown. The first vehicle flown carried two test wings, one of which fluttered at a Mach number of 0.92 at a frequency of 61.4 cycles per second. The reference flutter speed determined from two-dimensional theory for an unswept wing in incompressible flow is conservative when compared to the experimental flutter speed. This agrees with data obtained from previous rocket-propelled model and freely-falling-body tests.

The second vehicle also carried two test wings, one of which failed at a Mach number of 0.71 because of a low-frequency (9.6 cycles per second) divergent oscillation. Since this failure was not caused by conventional flexure-torsion flutter, no comparison with a reference flutter speed can be made.

INTRODUCTION

To obtain information on wing flutter at transonic speeds the NACA is conducting free-flight flutter tests using low-acceleration rocket-propelled vehicles. These vehicles are equipped with wings whose physical characteristics and flutter parameters are determined before flight testing. The first of this series, designated as the NACA FR-1-A (flutter rocket - type 1 - model A), reported in reference 1, was equipped to measure only wing failure speed. The second, model B (reference 2), was equipped to measure wing failure speed, the torsional frequency of both wings, and the longitudinal acceleration.

Previous tests have shown that after the failure of one wing the model goes into a helical flight path and the other wing stays on for the remainder of the flight. Since it is desirable to obtain both torsion and bending frequencies on a flutter wing, and since the telemeter was limited to two strain channels, it was decided to put both bending and torsion gages on one wing. This wing was slotted to make it less rigid than the other so that it would be reasonably certain to flutter first and the desired data could be obtained.

Model D was instrumented to measure torsional frequency on both wings and bending frequency on one. The wings on this model were designed to have approximately the same section parameters as the wings of model C but had a larger aspect ratio and a much lower bending torsion frequency ratio.

Both tests were conducted at the Pilotless Aircraft Research Division test station, Wallops Island, Va., and the results are presented herein.

APPARATUS AND METHODS

Model

The test vehicles were rocket-propelled vehicles similar to models A and B. The test wings of model C were constructed of laminated spruce and the left wing slotted along the chord to give the desired torsional frequency. After slotting, the wing was covered with a thin layer of fabric. A sketch of these wings is shown in figure 1. The test wings of model D were constructed of laminated white pine with an inlay of 0.032-24ST duralumin. A sketch of these wings is shown in figure 2. A photograph of each model on the launching rack is shown in figure 3.

Model C was powered by a rocket motor delivering approximately 950 pounds of thrust for 15 seconds. The rocket motor in model D had a modified nozzle insert and delivered about 1140 pounds of thrust for 12 seconds.

Instrumentation

Telemeter.- The telemeter in model C consisted of two strain-gage channels and two inductance channels. The strain-gage channels were used to record torsional and bending frequencies by the use of strain variations on the surface of the wing. One inductance channel was used to record signals from a longitudinal accelerometer and the other was so connected to a breakwire routed through the left wing that the breaking of the wire would shift the frequency and thus determine the time of failure even if the wing broke outboard of the strain gages. The positions of the strain gages and breakwire are shown in figure 1.

The telemeter in model D was similar to that in the model C but with two additional channels. An additional strain-gage channel was used to pick up torsional frequency on the right wing and an additional inductance channel connected to a pressure pickup was used to record total-head pressure as a check of the airspeed determined from the longitudinal accelerometer.

Cameras and radar.- The camera installations were similar to those used in reference 1, consisting of fixed wide-angle aerial cameras and motion-picture cameras. In addition to the continuous wave Doppler radar, a tracking radar was used to obtain a more accurate altitude record of the flight.

Radiosonde.- A radiosonde was released immediately after the flight to determine atmospheric conditions prevailing at that time. The data obtained are shown in figure 4 as a plot of the velocity of sound and density of air against altitude.

Launching Technique

The method of launching was the same as that used for other NACA FR-1 models and is reported in reference 1. The launching angle of the model C was 63° and that of the model D was 60°.

RESULTS AND DISCUSSION

Flight data of the models C and D are shown in figures 5, 6, and 7 as variation of altitude, acceleration, velocity, and Mach number with time. The airfoil parameters of the wings are listed in table I. Conditions at the time of flutter, failure, or maximum speed are listed in table II.

The telemeter record (fig. 8) of model C flight shows that the left wing fluttered at a frequency of 61.4 cycles per second. This flutter occurred at a Mach number of 0.92, which corresponds to a velocity of 707 miles per hour, and the wing failed at a Mach number of 0.96, which corresponds to a velocity of 735 miles per hour. Using the two-dimensional, two-degree-of-freedom (first bending and uncoupled first torsion) theory of reference 3 and the air density at test conditions, the flutter frequency for the left wing was calculated to be 72.6 cycles per second and the flutter speed 558 miles per hour. When the experimental flutter speed is compared with the value calculated from the theory, it is seen that the experimental value exceeds the calculated by 26 percent. This percentage is in approximate agreement with those reported for unswept wings in references 4, 5, and 6.

Since there was no instrumentation on the right wing of model C, it is not possible to state definitely that the wing did not flutter or fail. However, movies taken of the flight and visual observation indicate that the wing remained on the model for the duration of the flight.

The telemeter record (fig. 9) of the model D flight shows that the left wing remained on the model throughout the flight and the right wing failed at a Mach number of 0.71, which corresponds to a speed of 542 miles per hour, after it had gone into a divergent oscillation whose frequency was 9.6 cycles per second. This frequency was about one-half the first bending frequency of the wing. Motion pictures showed that the model was pitching prior to failure. The wing did not fail due to the conventional flexure-torsion flutter of reference 3 and failure is believed to have been caused by an oscillation involving flexure of the wing and pitch of the model. Some of the mass and stability parameters of the model D are listed in table III.

CONCLUDING REMARKS

Data on flutter wings attached to two low-acceleration rocket vehicles have been presented. One wing on model C fluttered at a velocity of 707 miles per hour, Mach number equal to 0.92, at a frequency of 61.4 cycles per second. The speed calculated from the theory for two-dimensional unswept wings in incompressible flow is conservative when compared to the experimental flutter speed. This is in agreement with previous rocket and freely-falling-body tests of unswept wings.

The other wing on model C had no instrumentation but is not believed to have fluttered or failed.

The right wing on model D failed for reasons other than flexure-torsion flutter and the left wing remained on the model for the duration of the flight.

Langley Aeronautical Laboratory
National Advisory Committee for Aeronautics
Langley Field, Va.,

APPENDIX

SYMBOLS

c	airfoil chord perpendicular to leading edge, in.
l	airfoil length along leading edge outboard of body, in.
E.A.	distance of elastic axis of wing behind leading edge, percent chord
C.G.	distance of center of gravity of wing behind leading edge, percent chord
a	nondimensional elastic axis position $\left(\frac{2 \times \text{E.A.}}{100} - 1\right)$ (reference 3)
$a + X_\alpha$	nondimensional center-of-gravity position $\left(\frac{2 \times \text{C.G.}}{100} - 1\right)$ (reference 3)
${r_\alpha}^2$	square of nondimensional radius of gyration about elastic axis $\frac{I}{mb^2}$ where I is polar moment of inertia about elastic axis (reference 3)
M	Mach number
M_{cr}	theoretical Mach number at which sonic velocity is first attained over section of wing taken perpendicular to leading edge at zero lift
Λ	angle of sweep of mean aerodynamic chord positive for sweepback
ϕ	phase angle wing torsional strain leading wing bending strain, deg
A_g	aspect ratio of one wing panel $\left(\frac{(l \cos \Lambda)^2}{lc}\right)$
b	semichord in feet $\left(\frac{c}{2 \times 12}\right)$ (reference 3)
ρ	air density, slugs/cu ft

κ	weight ratio $\left(\frac{\pi \rho b^2}{m}\right)$, where m is the mass of the airfoil per unit length (reference 3)
p_s	static pressure, lb/sq ft
T	free-air temperature, $^{\circ}F$ absolute
t	time after firing, sec
q	dynamic pressure, lb/sq ft $\left(\frac{1}{2}\rho v^2\right)$
v	velocity, fps
V_e	model velocity at start of wing flutter, mph
V_{max}	maximum velocity attained by wing, mph
h	geometric altitude, ft
GJ	torsional rigidity, lb-in.^{2}
EI	bending rigidity, lb-in.^{2}
g_h	structural damping coefficient in bending (reference 3)
g_{α}	structural damping coefficient in torsion (reference 3)
f_e	experimental wing-flutter frequency, cps
f_{h_1}	first bending natural frequency, cps
f_{h_2}	second bending natural frequency, cps
f_t	first torsion natural frequency, cps
f_{α}	first torsion frequency (uncoupled) about elastic axis, cps
V_R	reference wing-flutter velocity perpendicular to leading edge, mph (based on theory for two-dimensional unswept wing in an incompressible medium employing first bending frequency and uncoupled torsion frequency and density of testing medium at time of beginning of flutter (reference 3)
f_R	reference wing-flutter frequency, cps (analysis similar to that used in determining V_R)

V_D reference wing-divergence speed, mph (based on theory for two-dimensional unswept wing in an incompressible medium employing uncoupled torsion frequency and density of testing medium at time of beginning of flutter (reference 3)

$\frac{v}{b\omega_\alpha}$ nondimensional flutter-velocity coefficient where $\omega_\alpha = 2\pi f_\alpha$ (reference 3)

REFERENCES

1. Angle, Ellwyn E.: Initial Flight Test of the NACA FR-1-A, A Low-Acceleration Rocket-Propelled Vehicle for Transonic Flutter Research. NACA RM No. L7J08, 1948.

2. Angle, Ellwyn E., Clevenson, Sherman A., and Lundstrom, Reginald R.: Flight Test of NACA FR-1-B, A Low-Acceleration Rocket-Propelled Vehicle for Transonic Flutter Research. NACA RM No. L8C24, 1948.

3. Theodorsen, Theodore, and Garrick, I. E.: Mechanism of Flutter - A Theoretical and Experimental Investigation of the Flutter Problem. NACA Rep. No. 685, 1940.

4. Barmby, J. G., and Clevenson, S. A.: Initial Test in the Transonic Range of Four Flutter Airfoils Attached to a Freely Falling Body. NACA RM No. L7B27, 1947.

5. Clevenson, S. A., and Lauten, William T., Jr.: Flutter Investigation in the Transonic Range of Six Airfoils Attached to Three Freely Falling Bodies. NACA RM No. L7K17, 1948.

6. Barmby, J. G., and Teitelbaum, J. M.: Initial Flight Tests of the NACA FR-2, A High-Velocity Rocket-Propelled Vehicle for Transonic Flutter Research. NACA RM No. L7J20, 1948.

TABLE I

WING PARAMETERS

Parameters	Airfoil Designation			
	FR-1-C Right	FR-1-C Left	FR-1-D Right	FR-1-D Left
NACA Section	65-009	65-009	65A006	65A006
M_{cr}	0.79	0.79	0.84	0.84
c	12	12	10.0625	10.0625
l	19.25	19.25	29.875	29.875
A_g.	1.6	1.6	3	3
Λ	0	0	0	0
b	0.5	0.5	0.419	0.419
C.G.	41.6	41.6	37.6	38.8
E.A.	34.4	37.5	35.2	33.5
a	-0.312	-0.25	-0.296	-0.33
$a + x_\alpha$. . . .	-0.168	-0.168	-0.248	-0.224
$1/\kappa$ (stnd.) .	28.3	28.3	25.1	24.6
r_α^2	0.23	0.24	0.2105	0.2255
f_{h_1}	78	55	20	19.5
f_{h_2}	425-500	300-350	115.5	115.0
f_t	145	105	138.5	134
f_α	135	102.5	137.5	131
GJ	244,000	186,600	361,000	336,000
EI	743,000	486,000	293,500	276,000
g_h		0.15		0.05
g_α		0.02	0.02	0.01

NACA RM No. L8I30

TABLE II

EXPERIMENTAL RESULTS

Parameter	FR-1-C Right (c)	FR-1-C Left (a)	FR-1-D Right (b)	FR-1-D Left (c)
M	0.970	0.920	0.710	1.11
V_e		707		
V_{max} . . .	755	743.5	542	839
ρ	0.00213	0.00216	0.002272	0.002143
q	1305	1165	718	1625
p_s	1961.4	1992.8	2039	1865.5
T	532	532	521.2	507
t	10.76	9.37	5.68	12
h	2280	1880	1200	3618
$1/\kappa$ . . .	31.6	31.15	26.3	27.3
ϕ		132°		
f_e		61.4		
f_R	101.3	72.6	64.2	65.8
V_R	750	558	751	687
V_D	1280	850	910	1005

NACA

[a]Conditions at time of flutter.

[b]Conditions at time of break.

[c]Conditions at time of maximum speed.

TABLE III

MASS AND STABILITY PARAMETERS OF MODEL D

Weight of model, lb	240
Center-of-gravity position, in. from nose	59
Leading edge of wing, in. from nose	76
Moment of inertia of complete model about the center of gravity, slug-ft^2	16

NACA

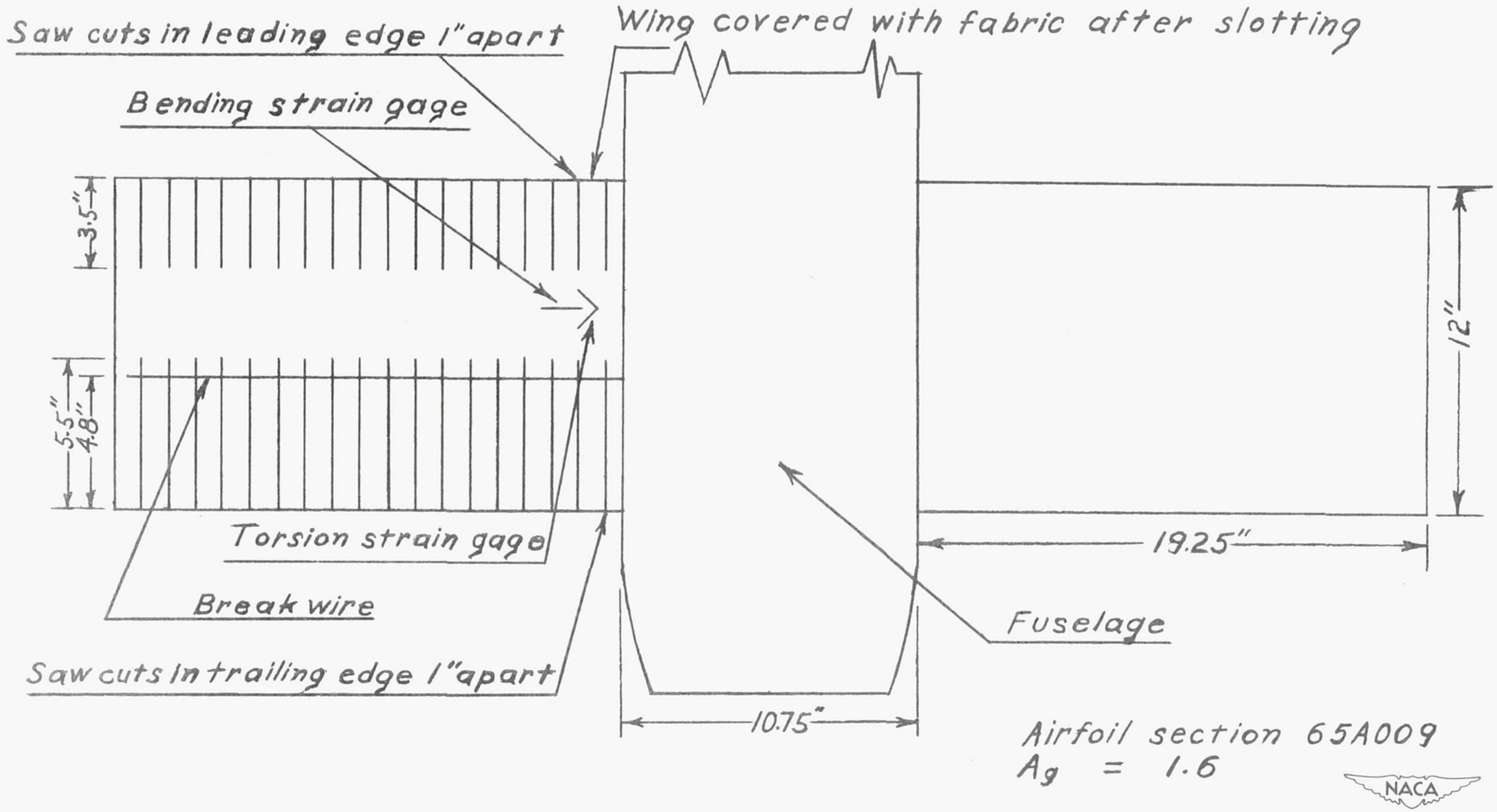

Figure 1.- Test wings of NACA FR-1-C.

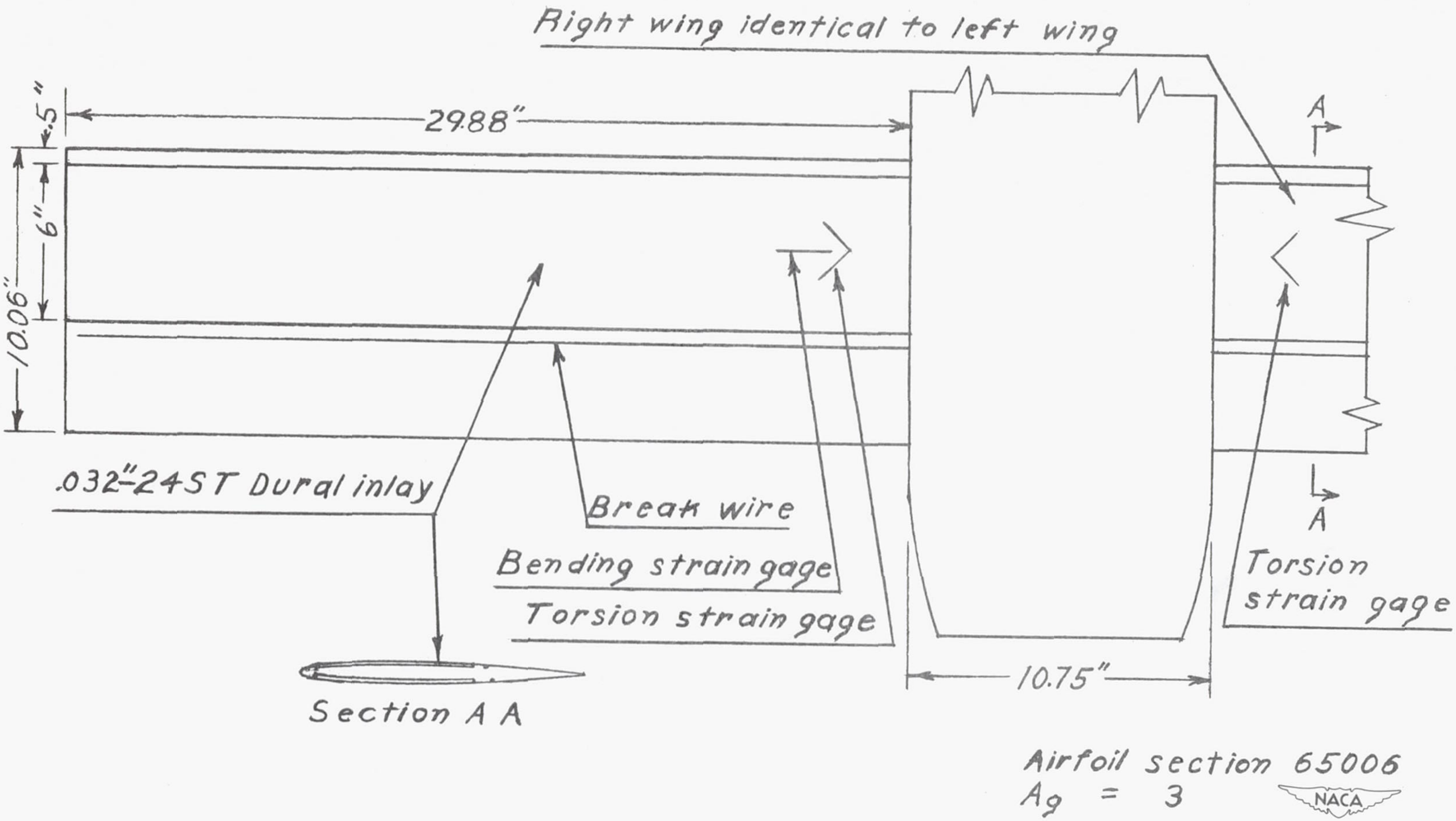

Figure 2.- Test wings of NACA FR-1-D.

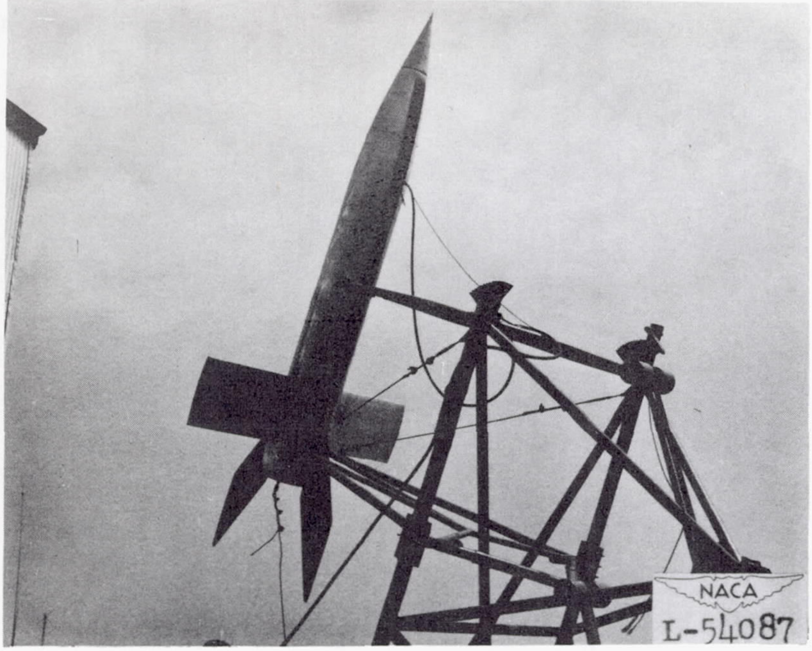

(a) Model C in position for launching.

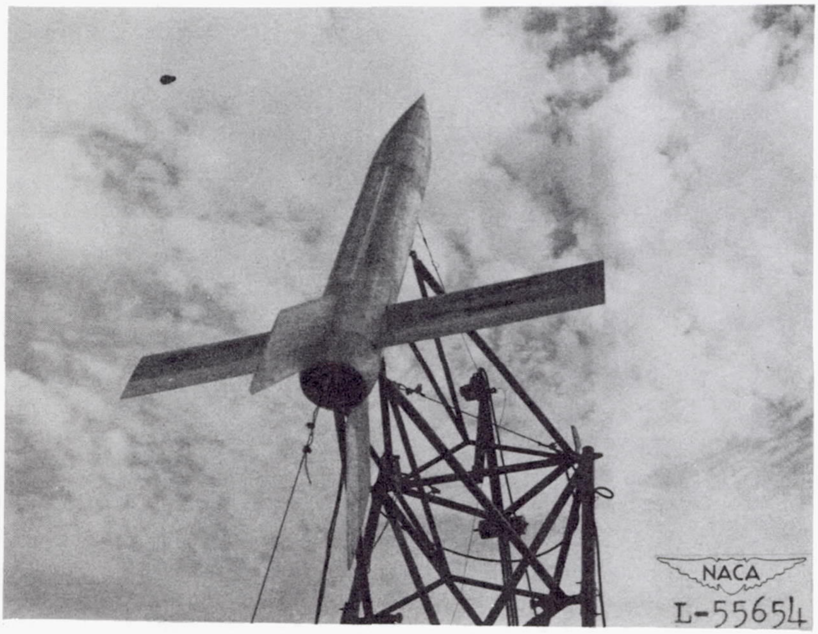

(b) Model D in position for launching.

Figure 3.- Launching positions of models.

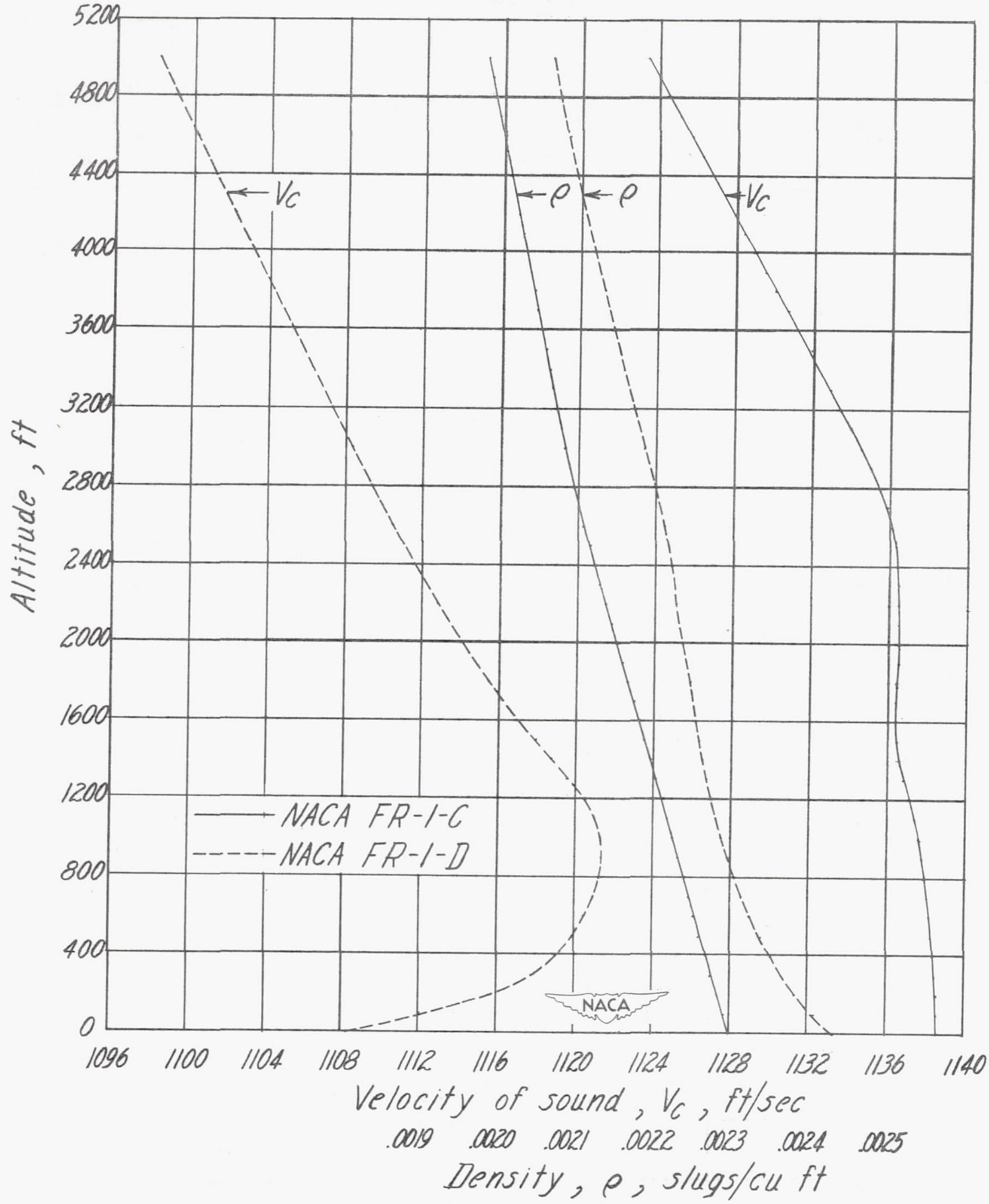

Figure 4.- Results of radiosonde records.

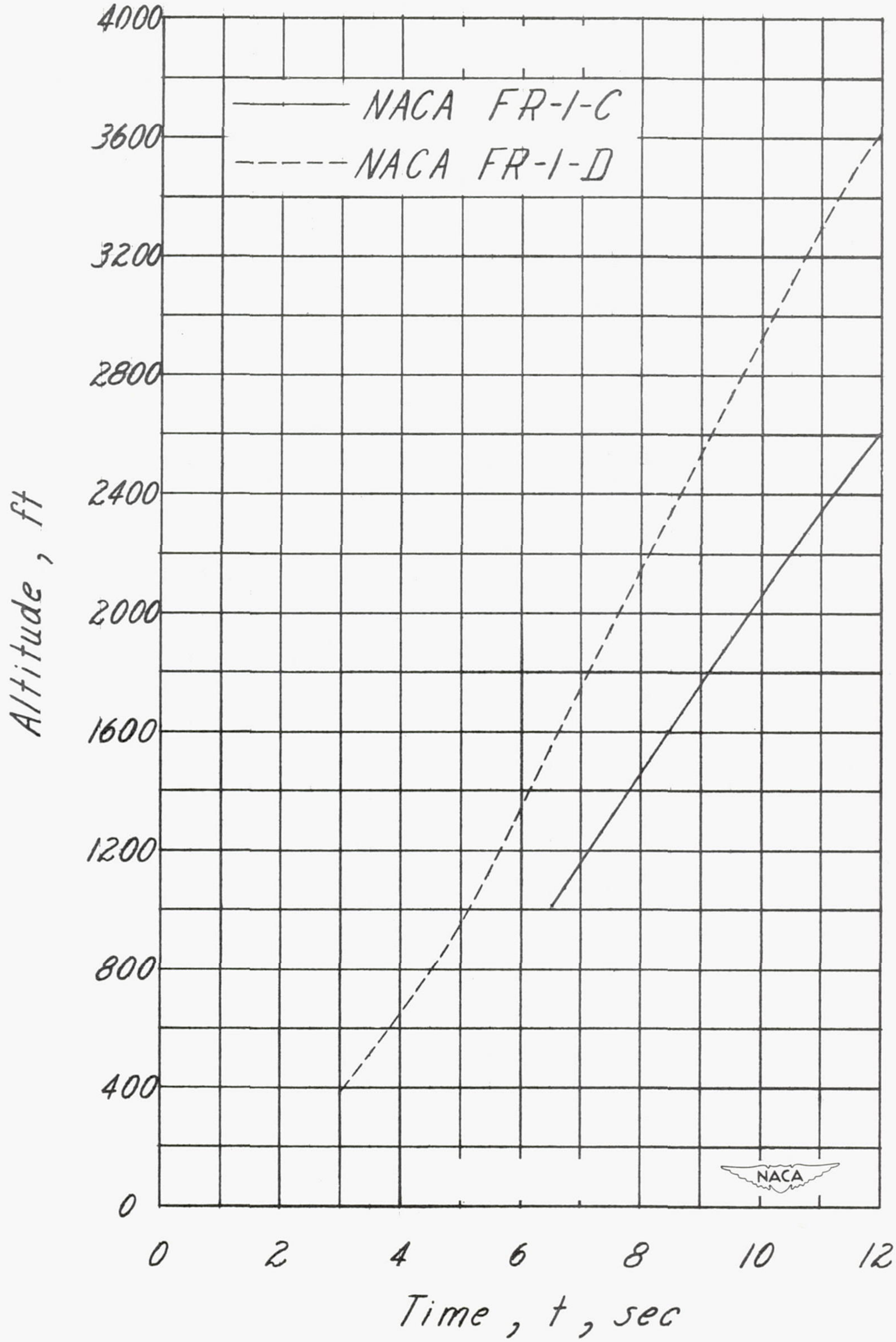

Figure 5.- Results of records from tracking radar.

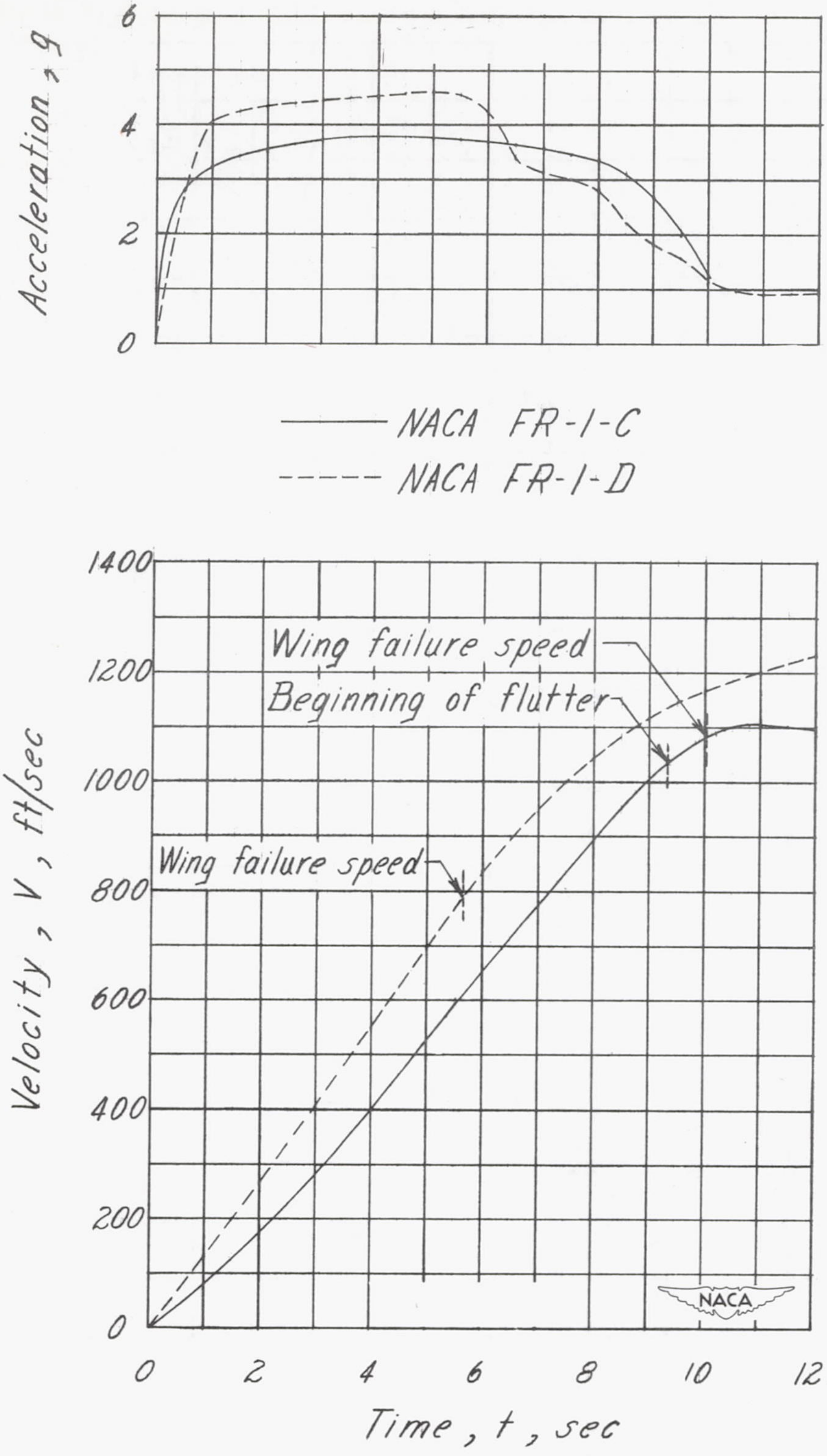

Figure 6.- Variation of acceleration and velocity with time.

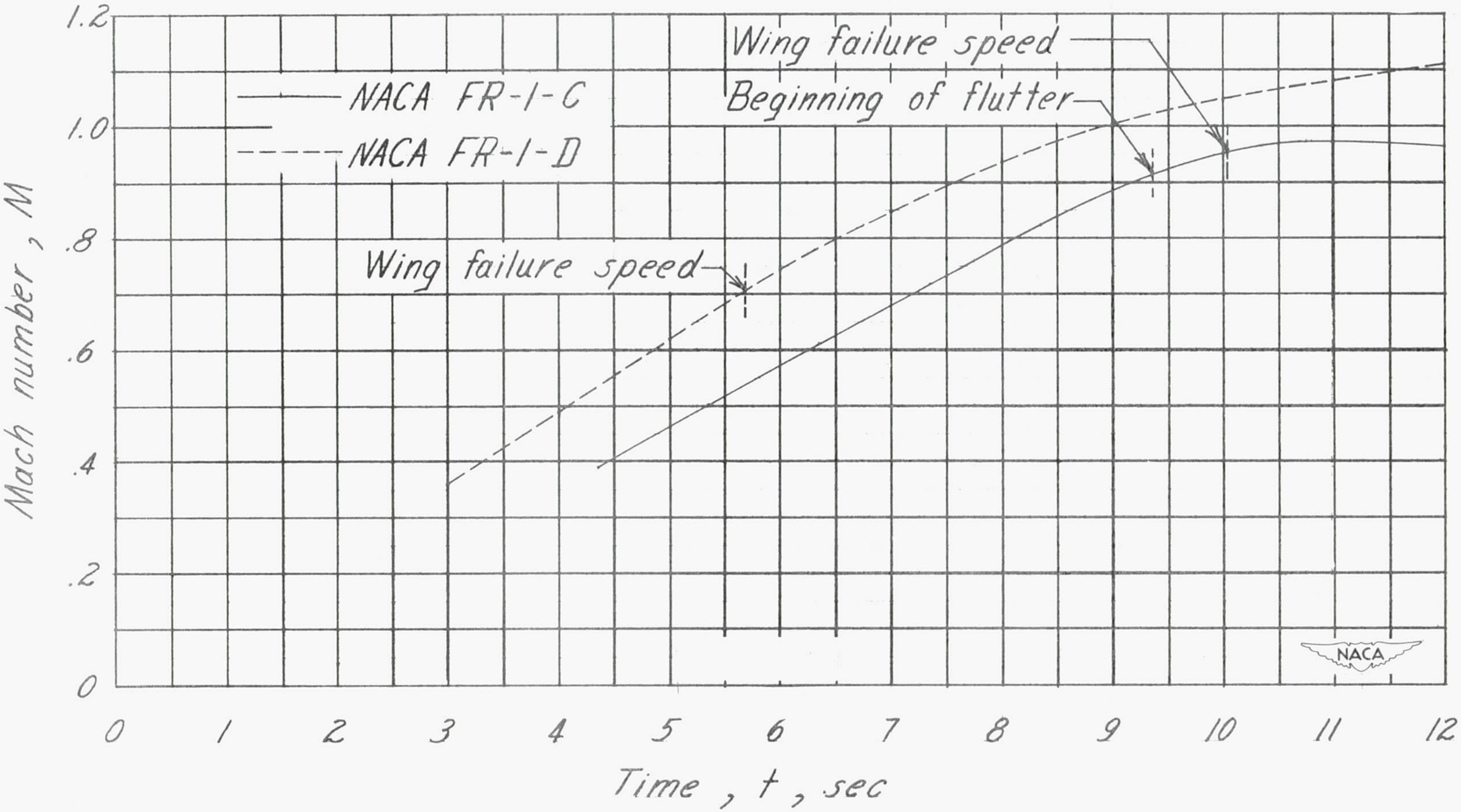

Figure 7.- Variation of Mach number with time.

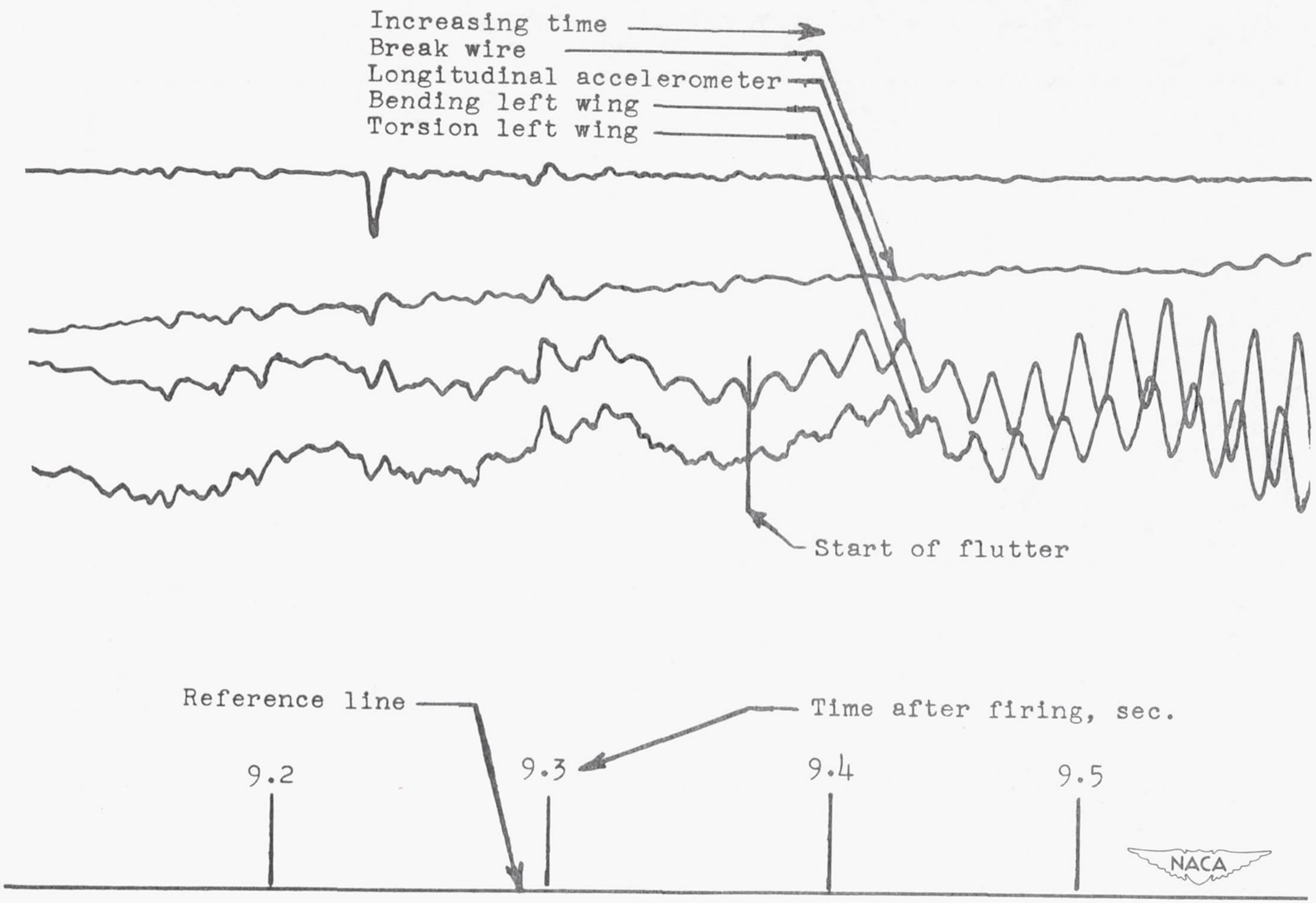

Figure 8.- Portion of telemetered record showing wing flutter, model C.

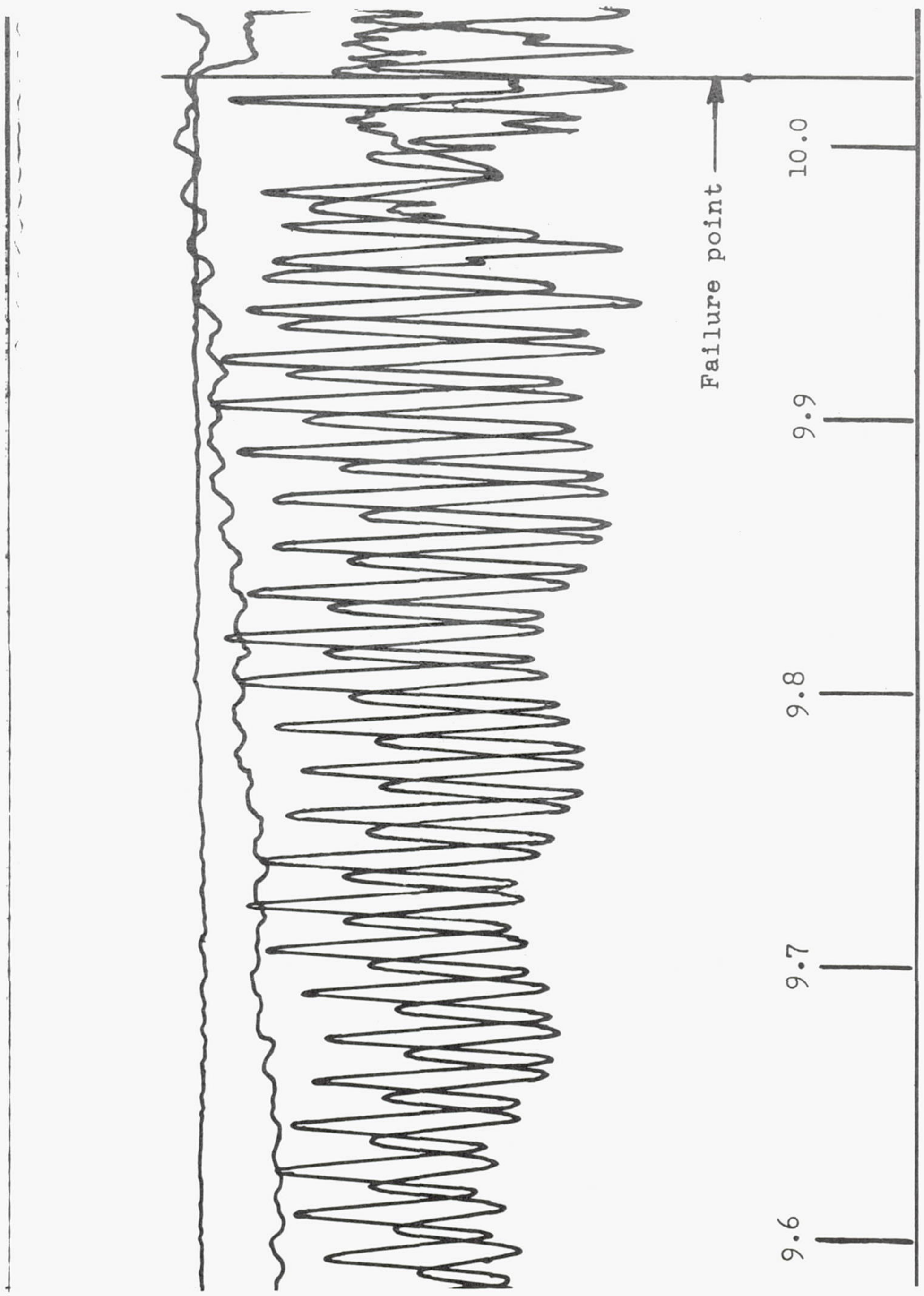

Figure 8.- Concluded.

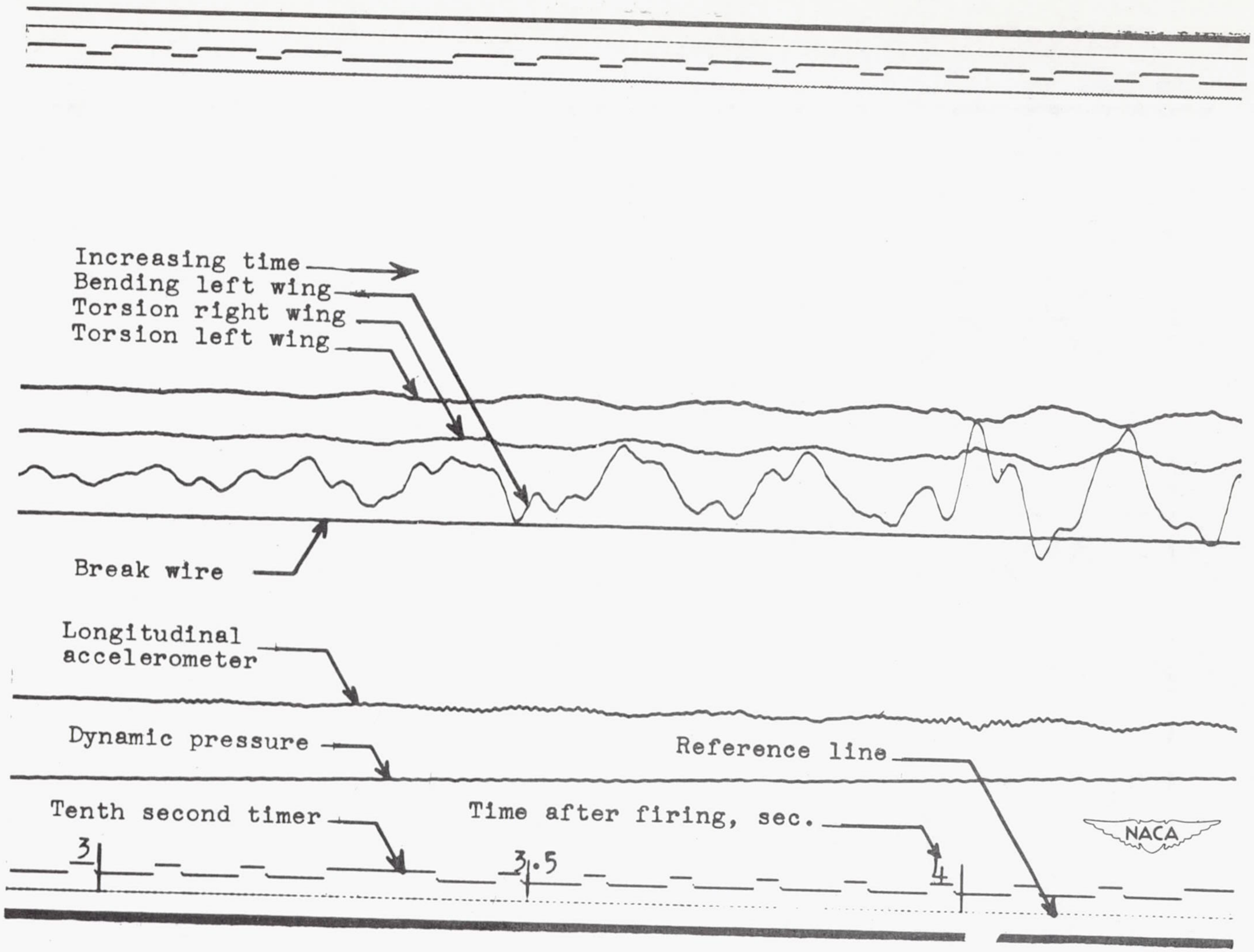

Figure 9.- Portion of telemetered record showing wing bending oscillations, model D.

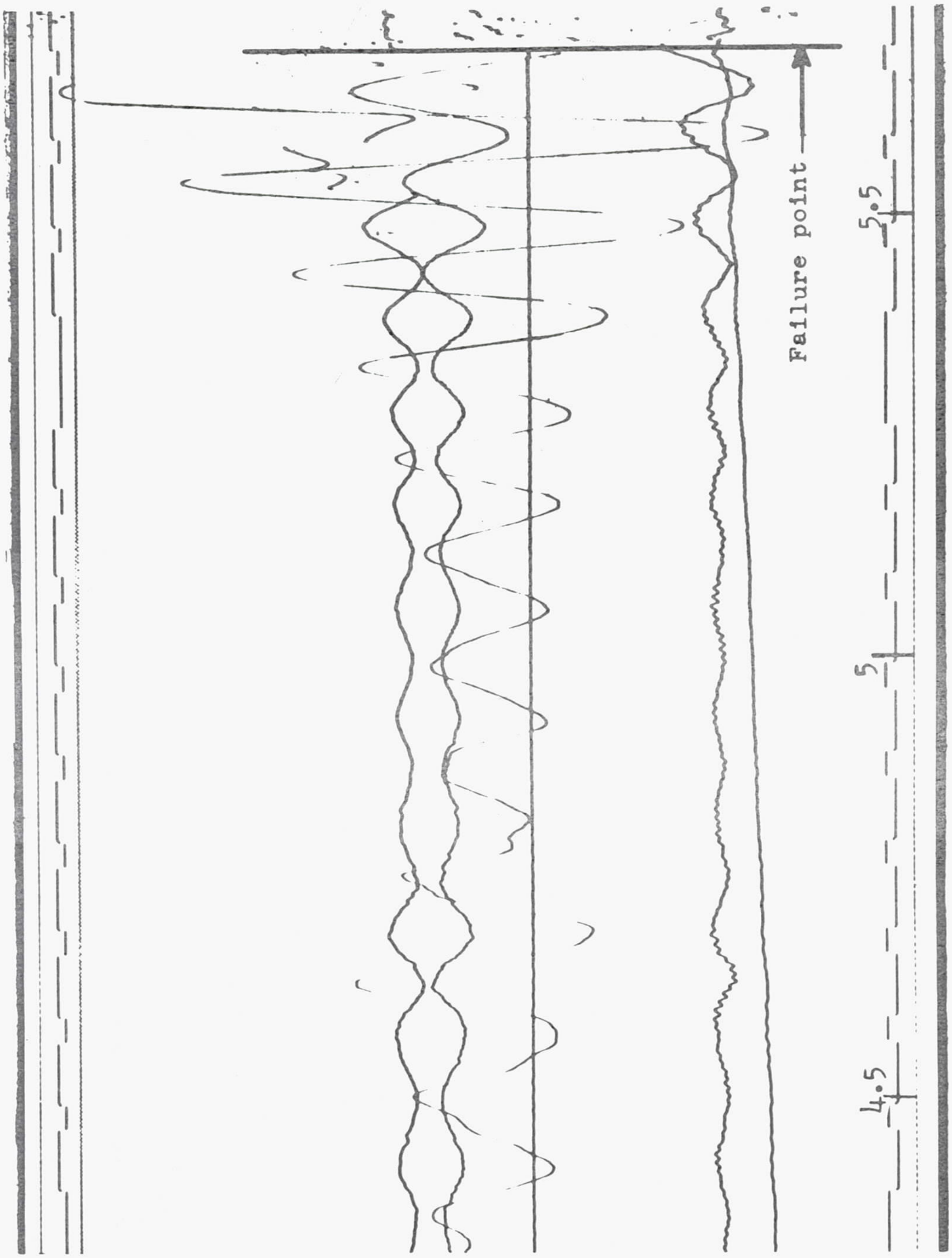

Figure 9.- Concluded.